JGR Atmospheres

RESEARCH ARTICLE
10.1029/2019JD031272

Implementation and Evaluation of an Improved Lake Scheme in Beijing Climate Center Atmosphere-Vegetation Interaction Model

Bo Qiu[1,2], Anning Huang[1], Xueli Shi[3], Yongjiu Dai[4], Nan Wei[4], Weidong Guo[1], Weiping Li[3], Lazhu[5], Yanwu Zhang[3], Zhipeng Fu[1], and Xiaolu Ling[1]

[1]CMA-NJU Joint Laboratory for Climate Prediction Studies, School of Atmospheric Sciences, Nanjing University, Nanjing, China, [2]Jiangsu Provincial Key Laboratory of Geographic Information Science and Technology, International Institute for Earth System Science, Nanjing University, Nanjing, China, [3]National Climate Center, China Meteorological Administration, Beijing, China, [4]Guangdong Province Key Laboratory for Climate Change and Natural Disaster Studies, School of Atmospheric Sciences, Guangzhou, China, [5]Key Laboratory of Tibetan Environment Changes and Land Surface Processes, Institute of Tibetan Plateau Research, Chinese Academy of Sciences, Bejing, China

Key Points:
- The default lake scheme in BCC_AVIM2.0 is replaced by the CoLM-Lake scheme
- Lake water temperature biases produced by the default lake scheme are largely reduced by adopting the CoLM-Lake scheme
- Large improvements in simulating lake ice are obtained by adopting the CoLM-Lake scheme in BCC_AVIM2.0

Correspondence to:
A. Huang,
anhuang@nju.edu.cn

Citation:
Qiu, B., Huang, A., Shi, X., Dai, Y., Wei, N., Guo, W., et al. (2020). Implementation and evaluation of an improved lake scheme in Beijing Climate Center Atmosphere-Vegetation Interaction Model. *Journal of Geophysical Research: Atmospheres*, *125*, e2019JD031272. https://doi.org/10.1029/2019JD031272

Received 30 JUN 2019
Accepted 4 APR 2020
Accepted article online 17 APR 2020

Abstract To improve the performance of the second generation of Beijing Climate Center Atmosphere-Vegetation Interaction Model (BCC_AVIM2.0) with a fine resolution (~45 km) over lake-rich areas, the default lake scheme in BCC_AVIM2.0 is replaced by the Common Land Surface Model (CoLM)-Lake scheme with much more realistic treatments of the energy exchanges in the snow-ice-water-sediment system relative to the default lake scheme. Results show that the lake surface temperature (LST) biases produced by BCC_AVIM2.0 with the default lake scheme can be largely reduced by adopting the CoLM-Lake scheme in winter due to much more realistically simulated vertical water temperature profiles over the Great Lakes region. The spatial distributions and seasonal variations of the LST simulations can also be significantly improved by the CoLM-Lake scheme within BCC_AVIM2.0. The performances of BCC_AVIM2.0 in simulating the lake ice in winter can be largely improved by replacing the default lake scheme with the CoLM-Lake scheme. The improvements in the LST simulated by BCC_AVIM2.0 with the CoLM-Lake scheme further lead to reduced biases in the simulated ground surface temperature. The simulations of air temperature and precipitation in the coupled model are also improved by adopting the CoLM-Lake scheme over the Great Lakes region, which indicates the improvements in simulating the energy and water exchange between the atmosphere and lakes. This study highlights the importance of a more realistic lake scheme in simulating the ground surface temperature and the energy exchanges between the atmosphere and lakes.

1. Introduction

The Beijing Climate Center Climate System Model (BCC-CSM) has been developed for seasonal climate predictions and future climate projections during recent decades (Wu et al., 2010, 2013, 2014; Xin et al., 2013). As the land component of this model, Beijing Climate Center Atmosphere-Vegetation Interaction Model (BCC_AVIM) was developed based on the National Center for Atmospheric Research (NCAR) Community Land Model version 3 (CLM3) model and the second version of Atmosphere-Vegetation Interaction Model (AVIM2; Ji, 1995; Ji et al., 2008). The first generation of BCC_AVIM (BCC_AVIM1.0) is the land surface component in BCC-CSM1.1 and BCC-CSM1.1(m), which have been contributed to the Coupled Model Intercomparison Project phase five (CMIP5) in support of the Intergovernmental Panel on Climate Change Fifth Assessment Report (Xin et al., 2013). After the CMIP5 experiments, several improvements of the parameterization schemes have been conducted in the second generation of this model (BCC_AVIM2.0), which is used for the ongoing CMIP6 (Li et al., 2019; Wu et al., 2019a).

The ground surface temperature (GST) plays an important role in the land-air interactions for climate system models. The modeled GST has substantial impacts on the turbulent fluxes of latent and sensible heat, which are important physical processes that influence the energy and water exchange between the atmosphere and land surface (Charusombat et al., 2018). For the lake-rich regions, the sensible heat flux

between the atmosphere and lakes may lead to strong convection during early winter, while evaporation (latent heat flux) from the lakes is the primary source of water vapor for precipitation formation (Sharma et al., 2018). In BCC-CSM2.0, the annual mean air temperature is colder than that in the European Centre for Medium-Range Weather Forecasts Reanalysis (ERA)-Interim reanalysis over the Great Lakes region (Wu, Huang, et al., 2019). Moreover, similar cold biases existed in the previous versions of BCC-CSM (Wu et al., 2014). The consistent colder temperature simulated by BCC-CSM in the lake-rich regions may associate with the lake scheme. The default lake scheme in BCC_AVIM2.0 is identical to that in the NCAR CLM version 2 (Bonan et al., 2002; Zeng et al., 2002), which is developed based on the scheme of Hostetler and Bartlein (1990). In the existing default lake scheme, all lake depths are fixed to 50 m and the treatments of snow above the ice and soil in the lake sediment are not considered. Due to the simple and unrealistic assumptions, the default lake scheme cannot accurately describe realistic lake physical processes and has large bias in the descriptions of lake physical processes (Li et al., 2019). Therefore, the temperature and precipitation simulated by BCC-CSM may have large bias due to the unrealistic assumptions of the lake scheme over the lake-rich regions.

Substantial improvements have been achieved in the developments of lake schemes during recent decades. Three kinds of one-dimensional (1-D) lake models have been developed to simulate lake thermodynamics: (1) the Freshwater Lake (FLake) model, which is a relatively simple two-layer model based on similarity theories (Gula & Peltier, 2012; Mallard et al., 2014; Mironov et al., 2010); (2) the thermal diffusion models based on an eddy diffusivity parameterization (Hostetler model, Hostetler & Bartlein, 1990; Stepanenko et al., 2010); and (3) the multilayer thermodynamic models (Goyette et al., 2000; Subin et al., 2012). These 1-D lake schemes have been implemented into land surface models. For example, Dai et al. (2018) developed a new lake scheme to simulate lake thermodynamics, and this improved lake scheme has been implemented into the latest version of the Common Land Surface Model (CoLM). The CoLM-Lake scheme has large improvements in the freezing and thawing processes; parameterizations of lake surface properties; spatially variable prescribed lake depth; and heat exchanges among snow, ice, water, and soil in the lake sediment. The water temperature simulations from the CoLM-Lake scheme were evaluated by the observations from 10 lakes over different regions across the globe, and the results demonstrated that the CoLM-Lake scheme was suitable for the simulation of lake physical processes (Dai et al., 2018). Huang et al. (2019) evaluated the model performances of the FLake, WRF-Lake, and CoLM-Lake models and demonstrated the good ability of the CoLM-Lake scheme in simulating the thermal features and vertical water temperature profile.

In this study, we incorporated the CoLM-Lake scheme into BCC_AVIM2.0 to replace the default lake scheme and evaluated its impacts on the model performances in simulating the seasonal variations of lake surface temperature (LST), water temperature profile, and the GST over the Great Lakes region. The two main goals of this study are as follows: (1) to improve the ability of BCC_AVIM2.0 by adopting the CoLM-Lake scheme instead of the default lake scheme in simulating the lake thermal features and thereafter GST over the Great Lakes area; (2) to investigate how the CoLM-Lake scheme improve the simulations of the lake physical processes compared to that from the default lake scheme. Findings of this study may provide valuable information for further calibrations and improvements of the lake scheme in BCC_CSM with much finer horizontal resolution in the future.

2. Materials and Methods

2.1. Data

The Great Lakes contain one fifth of the world's surface freshwater supplies and play a critical role in influencing hydrological systems and regional climate patterns throughout North America (Norton & Bolsenga, 1993; Notaro et al., 2013; Patz et al., 2008). The Great Lakes in North America, consisting of five huge lakes (Superior, Michigan, Huron, Ontario, and Erie), has a total water surface area of 245,000 km^2 (Huang et al., 2010). There are many observed and remotely sensed data sets with good quality in this area, and these data have been widely used for the developments and calibrations of lake schemes in climate models (Gu et al., 2015; Huang et al., 2010; Xiao et al., 2016). Therefore, the Great Lakes region is chosen as the study area to evaluate the spatial and temporal variations of LST simulated by BCC_AVIM2.0. The Great Lakes region (40–50°N, 75–93°W) is defined as the lake areas (Lake Superior, Michigan, Huron, Erie, and Ontario) and their surrounding regions.

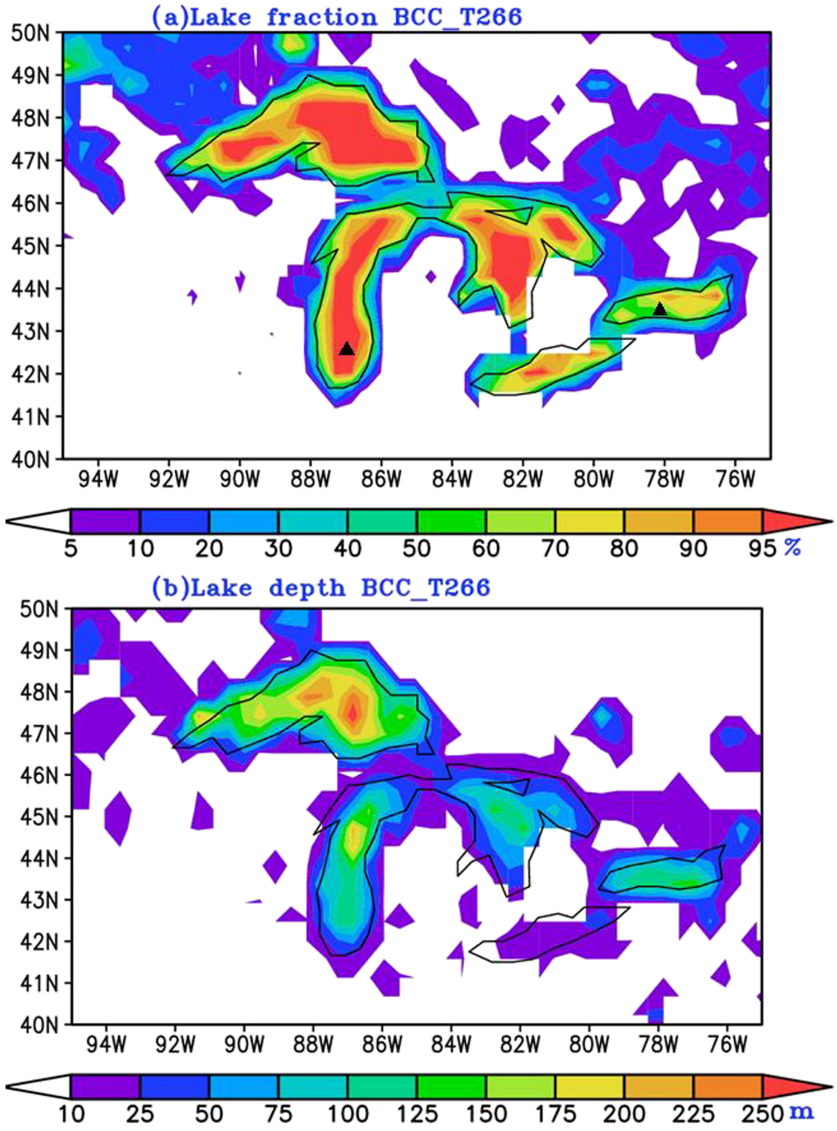

Figure 1. The (a) lake fraction and (b) depth over the Great Lakes area with the horizontal resolution of T266 and the mooring stations in Lake Michigan (CM1) and Ontario (403) marked by dark triangles in (a).

Lake depth is an important parameter in lake schemes. The lake depth data from the Global Lake Database (GLDB) are widely adopted for the lake parameterization development in climate models (Choulga et al., 2014). These gridded lake depth data (http://www.flake.igb-berlin.de/ep-data.shtml) with a horizontal resolution of 30 s (~1 km) are adopted in this study. The GLDB is used to locate lakes on the globe and to discriminate between the lake pixels and the nonlake pixels. In addition, BCC_AVIM2.0 is run with the fine resolution of T266 (~45 km). To match the model resolution, the lake depth (mean subgrid lake depth on a grid) and lake fraction (the ratio of subgrid lake areas to the total area on a grid with the unit of %) with the model resolution of T266 (~45 km) are derived from the GLDB data (Figure 1).

The atmospheric forcing data from the Princeton University Hydroclimatology Group Bias Corrected Meteorological Forcing Dataset (Sheffield et al., 2006), which were developed for land surface modeling, are used to drive BCC_AVIM2.0 in this study. The atmospheric forcing data include air temperature at 2 m above ground, specific humidity, and wind speed at 10 m above ground, downward shortwave and long-wave radiation at surface, surface air pressure, and precipitation (http://hydrology.princeton.edu/data/pgf/v1/1.0deg/3hourly/).

The observational data sets are also collected to evaluate the model simulations in this study. The observed daily LST over the Great Lakes region from 1995 to 2006 are collected from the National Oceanic and Atmospheric Administration Great Lakes Surface Environmental Analysis (GLSEA) data (Schwab et al., 1992). The GLSEA data are derived from the cloud-free portions of the previous day's satellite imagery. A smoothing algorithm is used to generate continuous daily LST data when no imagery is available. The GLSEA daily mean LST data (ftp://coastwatch.glerl.noaa.gov/glsea/asc_1024/) at a spatial resolution of ~1 km are adopted in this study. The lake ice fraction data over the Great Lakes are collected from the Great Lakes Environmental Research Laboratory (GLERL) to evaluate the spatial distribution of lake ice cover over the Great Lakes. The GLERL daily data (available from http://www.glerl.noaa.gov/data/ice) at a spatial resolution of ~2.55 km are adopted for the period of 1999–2006 in this study.

The GST and air temperature at 2 m reanalysis data from the ERA-Interim reanalysis are also used in this paper. The monthly mean GST and air temperature data sets at a spatial resolution of 0.5° are available at https://apps.ecmwf.int/datasets/data/. The Global Precipitation Climatology Project (GPCP) data set is obtained from the World Climate Research Program/Global Water Cycle and Energy Experiment. GPCP data sets, which are retrieved from global satellite data and gauge observations, have been widely used to evaluate the precipitation simulations from climate models (Adler et al., 2003). The monthly GPCP data sets at a spatial resolution of 2.5° are available at http://gpcp.umd.edu/.The moored thermistor can measure water temperatures at different depths and provide a site-specific vertical temperature profile to evaluate the model performance in simulating vertical thermal structure. Here we use the daily mean water temperature profiles observed in Lake Ontario (Huang et al., 2010) and Lake Michigan (Xiao et al., 2016) for model evaluation (Figure 1).

2.2. Model Description and Experimental Design

2.2.1. BCC_AVIM2.0 Land Surface Model

The BCC_AVIM2.0 land surface model consists of physiological, biophysical, and soil carbon-nitrogen dynamical processes. Compared to those in BCC_AVIM1.0, several improvements of the parameterization schemes have been conducted in BCC_AVIM2.0 (Wu et al., 2019a). For example, the default two-stream method in BCC_AVIM1.0 cannot accurately describe the realistic radiative transfer process within the canopy due to the several assumptions in simplifying the governing equations (Qiu et al., 2016), and then a four-stream approximation on solar radiation transfer within the canopy is implemented in BCC_AVIM2.0 (Zhou et al., 2018). In addition, an improved scheme of snow age and snow surface albedo is adopted by BCC_AVIM2.0 to describe the different reduction rates of snow albedo in the accumulating and melting stages in snow seasons (Wu et al., 2019a).

2.2.2. Lake Scheme

The governing equation for the 1-D Lake scheme (Hostetler & Bartlein, 1990) is given by

$$\frac{\partial T}{\partial t} = \frac{\partial}{\partial z}\left[K_w \frac{\partial T}{\partial z}\right] - \frac{1}{c_w}\frac{d\phi}{dz}, \tag{1}$$

where T, t, z, K_w, ϕ, and c_w are water temperature (K), time (s), depth from the surface (m), the eddy diffusion ($m^2\ s^{-1}$), a heat source term ($W\ m^{-2}$), and the volumetric heat capacity ($J\ m^{-3}\ K^{-1}$), respectively. Compared to the default lake scheme in BCC_AVIM2.0, several lake properties and physical processes have been improved in the CoLM-Lake scheme. The modifications include model vertical structure, extinction coefficient, lake surface albedo, and surface roughness lengths.

The schematic diagram of the model vertical structure in the default lake scheme is shown in Figure 2a. All lakes are “deep” lakes with the depth fixed to 50 m. The default lake scheme solves the 1-D thermal diffusion equation by dividing the vertical profile into 10 layers of water and ice. In addition, the treatments of snow above the ice and soil in the lake sediment are not considered in the default lake scheme.

The CoLM-Lake scheme solves the 1-D thermal diffusion equation by dividing the snow-ice-lake-soil vertical profile into several discrete layers: up to 5 snow layers above the lake ice based on the snow depth, 10 layers of water and ice, and 10 soil layers in the bottom lake sediment (Figure 2b). The lake depth is variable with global distributions of lake depth used in the CoLM-Lake scheme. The treatment of snow in CoLM-Lake is nearly identical to the snow model used over the nonlake grids in CoLM (Dai et al., 2018).

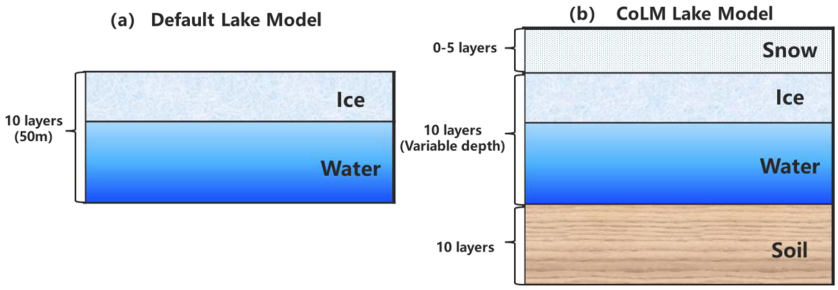

Figure 2. Schematic diagrams of (a) the default Llake model in BCC_AVIM2.0 and (b) the CoLM-Lake model.

When the snow thickness is less than a small threshold (0.01 m), snow only exists in the model without being represented by explicit snow layers. Once the snow thickness exceeds 0.01 m, snow can have up to five layers, and the number of snow layers varies according to the snow depth (Dai et al., 2003). The treatments of soil in the lake sediment are similar to the CoLM soil module, but the soil moisture is saturated in the sediment layers beneath the lake. More details of the CoLM-Lake scheme description can be found in Huang et al. (2019).

2.2.3. Experimental Design

The performance of BCC_AVIM2.0 with the adoption of the default lake and CoLM-Lake schemes in simulating the lake thermal features and GST is evaluated and compared over the Great Lakes region. All the results in this work are based on the offline simulations of BCC_AVIM2.0. Table 1 shows the numerical experiment design. To evaluate the effects of the CoLM-Lake scheme on the performance of BCC_AVIM2.0 with the horizontal resolution of T266 (~45 km), three runs are carried out over the Great Lakes region. In the control run (referred to as CTL hereafter), the default lake scheme with all lake depths fixed to 50 m is adopted in BCC_AVIM2.0. In the CoLM-Lake run, the CoLM-Lake scheme is used to replace the default lake scheme in BCC_AVIM2.0, but all lake depths are still set to 50 m. In the CoLM-Lake_Dep run, real lake depths are used to examine the impacts of lake depth on the LST and GST simulations. The lake fractions (depths) for the three runs (CoLM-Lake_Dep run) are exhibited in Figure 1, which shows that the lake fractions (depths) over most areas in the Great Lakes region are larger than 80% (deeper than 100 m) at the horizontal resolution of ~45 km. Each run starts on 1 January 1980 and ends on 31 December 2006. We use the model results from 1995 to 2006 for analyses.

2.3. Method

In this study, two common statistical measures including spatial correlation coefficient (SCC) and root-mean-square error (RMSE) are adopted to quantify the spatial pattern similarity between observations and simulations and the model errors. The equations for these statistics are described as:

$$\mathrm{SCC} = \frac{\sum (s_i - \bar{s}) \cdot \sum (o_i - \bar{o})}{\sqrt{\sum (s_i - \bar{s})^2 \cdot \sum (o_i - \bar{o})^2}}, \tag{2}$$

$$\mathrm{RMSE} = \sqrt{\frac{\sum (s_i - o_i)^2}{N}}, \tag{3}$$

where s_i and o_i are time averaged values from respectively model outputs and satellite products for the ith grid and N is the number of grid points. A high value of SCC suggests a high similarity in the spatial pattern between the observation and simulation. A low RMSE indicates that the model simulations agree well with the observation in quantity. In addition, the Taylor diagram is used to validate the model simulations in the amplitude and pattern of variability simultaneously. The Taylor diagram can provide a concise statistical summary of how well patterns match each other in terms of their correlations and the ratio of their variances (Taylor, 2001).

Table 1
Numerical Experiment Design

Experiment	Lake model	Lake depth
CTL	Default	50 m
CoLM-Lake	CoLM-Lake	50 m
CoLM-Lake_Dep	CoLM-Lake	GLDB data

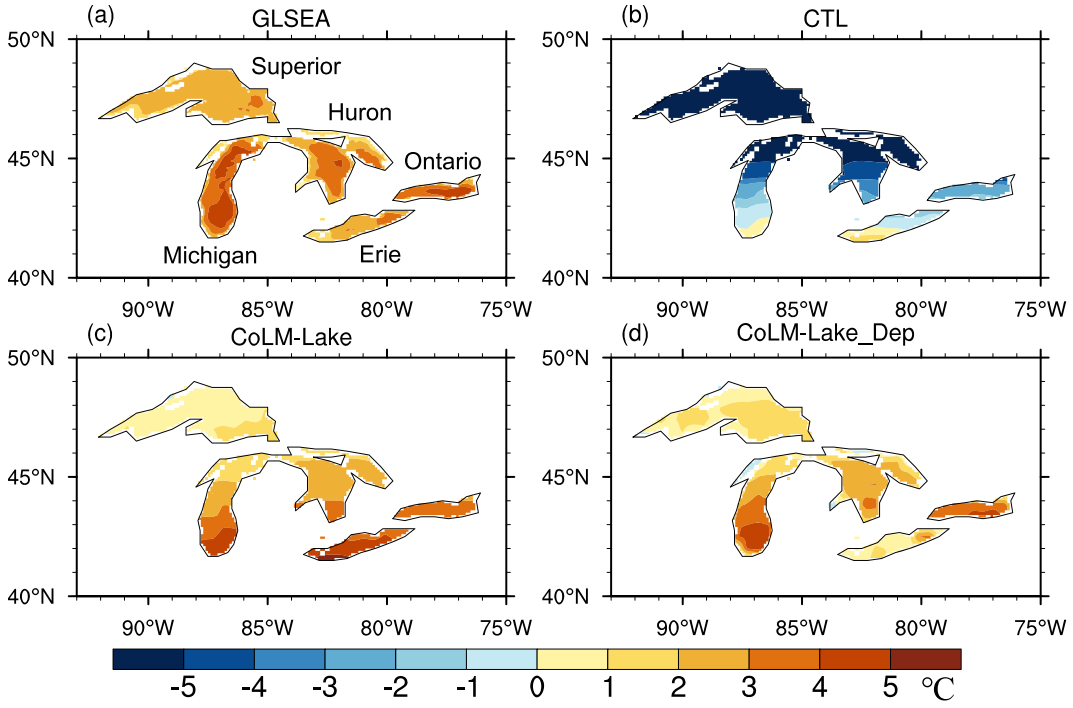

Figure 3. The observed and modeled lake surface temperature in winter (December, January, and February) averaged over 1995 to 2006. (a) GLSEA observation, (b) CTL, (c) CoLM-Lake, and (d) CoLM-Lake_Dep.

3. Results

3.1. Spatial Distributions of LST

Figure 3 gives the spatial distribution of the observed and modeled winter (December, January, and February) LST over the Great Lakes region in North America. For the GLSEA observations, the LST in winter is higher than 0 °C in most areas of the five lakes. The observed LST slightly increases from southern to northern lakes, with the lowest LST in Lake Superior and highest in the southern part of Lake Michigan. Besides, the lake depth also strongly affects the LST over the Great Lakes region. For example, the LST in the central part of Lake Michigan is higher than that along the lake shorelines. Moreover, the southern part of Lake Michigan has higher LST than has that of Lake Erie, which is the shallowest lake among the five lakes. In the CTL run, the winter LST increases with latitude from north to south. The values of modeled LST are much lower than that of the GLSEA observation and the largest biases are lower than −10 °C in Lake Superior (Figure 3b). The results from the CTL run indicate poor performance of BCC_AVIM2.0 with the default lake scheme in simulating the LST in winter. BCC_AVIM2.0 with the CoLM-Lake scheme can significantly improve the winter LST simulation over the Great Lakes region compared to the CTL run. Although the values in Lake Superior are still slightly lower, the modeled LST in the CoLM-Lake run is much closer to the observations compared to that in the CTL run. However, due to the fixed lake depth of 50 m in the CoLM-Lake run, the simulated LST in the central lake and along the shorelines are close to each other (Figure 3c). Compared to the simulations from the CoLM-Lake run, adopting the real lake depths in the CoLM-Lake_Dep run can further improve the spatial distributions of modeled LST in winter (Figure 3d). The spatial distributions of LST are similar in the CoLM-Lake and CoLM-Lake_Dep runs, but some distinct differences appear in Lake Erie, which is the shallowest lake among the five lakes. The realistic depth of Lake Erie is about 20 m (Figure 1), while the depth is 50 m in the CoLM-Lake run. The distinct differences between CoLM-Lake and CoLM-Lake_Dep indicate that the lake depth is an important parameter for the LST simulation. Overall, the implementation of the CoLM-Lake scheme within BCC_AVIM2.0 can remarkably improve the winter LST simulations.

As shown in Figure 4a, the observed LST in summer (June, July, and August) over the Great Lakes region exhibits large north-south gradients and much lower values in deep lakes than those in shallow lakes.

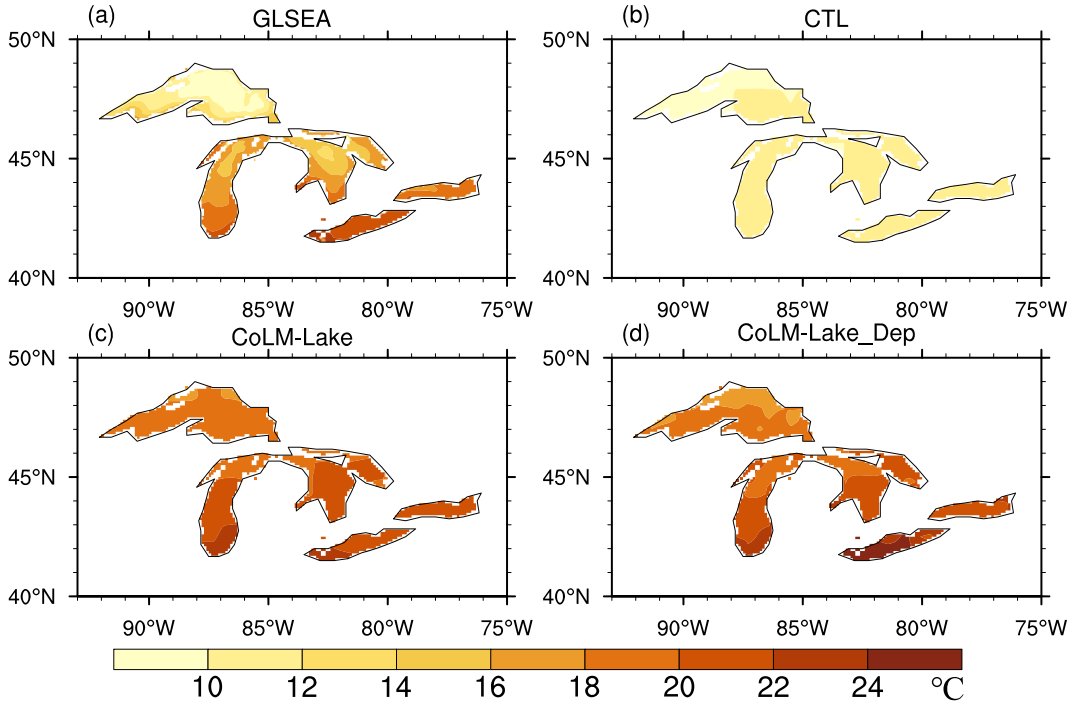

Figure 4. The observed and modeled lake surface temperature in summer (June, July, and August) averaged over 1995 to 2006. (a) GLSEA observation, (b) CTL, (c) CoLM-Lake, and (d) CoLM-Lake_Dep.

The lowest (highest) LST is located in the central Lake Superior (Erie) with the deepest (shallowest) water depth. In the CTL run, the modeled LST shows a widespread large cold bias relative to the GLSEA observation (Figure 4b), except for Lake Superior. The modeled LST is much higher in the CoLM-Lake run than in the CTL run in most of the lakes (Figure 4c). Large improvements can be found in most lakes (Erie, Ontario, Huron, and Michigan), but the warm biases are relatively large in the lakes at high latitudes, especially for Lake Superior. The CoLM-Lake_Dep run with the real lake depths can further slightly reduce the LST biases in deep lakes compared to the CoLM-Lake run (Figure 4d). Overall, the performances of BCC_AVIM2.0 in simulating the summer LST can be obviously improved by replacing the default lake scheme with the CoLM-Lake scheme.

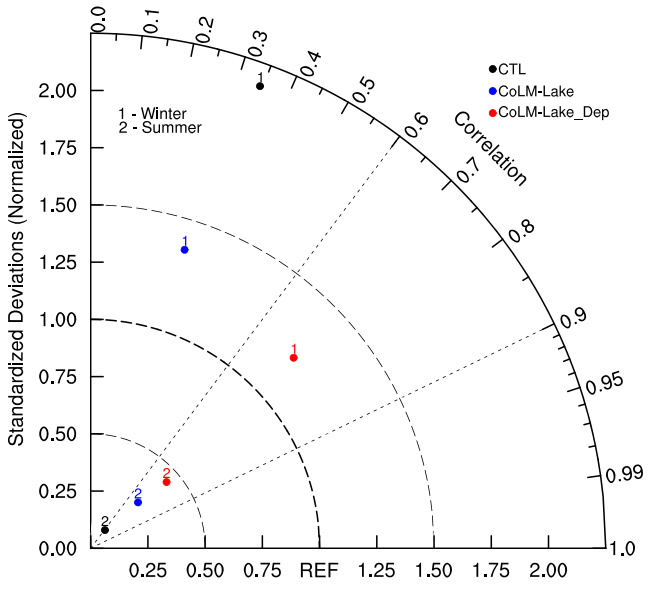

Figure 5. Taylor diagram of the climatic mean LST simulation against the GLSEA observation over the Great Lakes region. The winter and summer simulations are denoted by numbers; the black, blue, and red marks denote the simulations from the CTL, CoLM-Lake, and CoLM-Lake_Dep experiments, respectively.

To quantify the performance of each run in simulating the winter and summer LST, Figure 5 gives the multiple statistics of the simulated LST in the Taylor diagram. The CTL run shows very poor performance of LST simulations in winter, with the lowest SCC and largest RMSE among the three experiments. The RMSE of the CoLM-Lake run has a substantial reduction relative to that of the CTL run, indicating large improvements of the new lake scheme adopted in BCC_AVIM2.0. However, the SCC of winter LST in the CoLM-Lake run is close to that of CTL, indicating the substantial impacts of the lake depth on the simulation of winter LST in terms of spatial patterns. The RMSE of winter LST from the CoLM-Lake_Dep run decreases significantly, compared to that from CTL. In addition, the SCC in the CoLM-Lake_Dep run reaches 0.73, which significantly improves the ability of BCC_AVIM2.0 to simulate the spatial distributions of LST over the Great Lakes region. The results in summer are similar to those in winter, with the best LST simulations

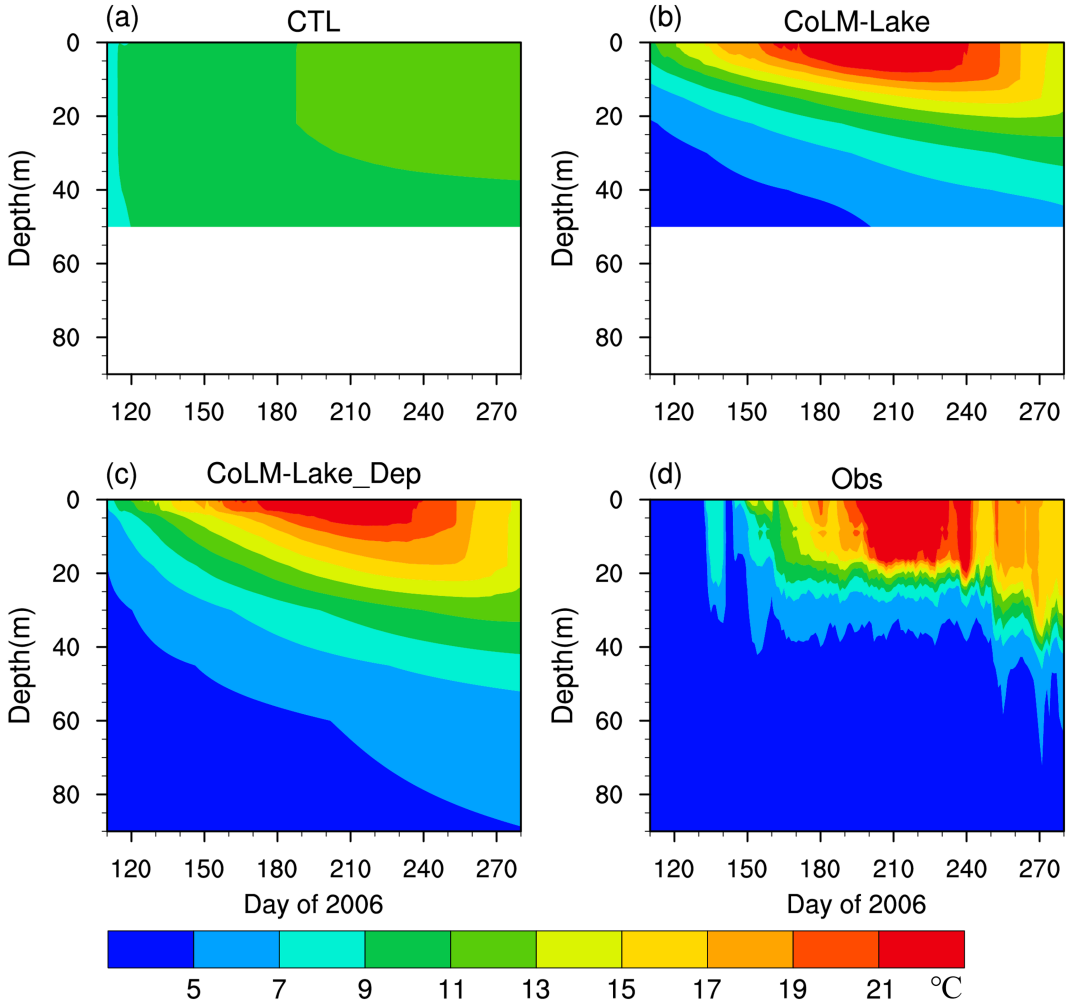

Figure 6. The modeled and observed daily vertical water temperature profiles (°C) in middle Lake Ontario during 2006: (a) CTL, (b) CoLM-Lake, (c) CoLM-Lake_Dep, and (d) observation.

in the CoLM-Lake_Dep run and the worst in the CTL run among the three runs. However, the improvements of the CoLM-Lake_Dep run are smaller in summer than in winter. Overall, adopting the CoLM-Lake scheme with the real lake depths can significantly improve the performance of BCC_AVIM2.0 to simulate the LST in terms of both magnitude and spatial pattern.

3.2. Lake Water Temperature

The seasonal variations of water temperature are examined in this part. Meanwhile, the vertical water temperature profiles from each experiment are also assessed against the mooring observations. The modeled water temperatures at different depths are interpolated on each depth of the thermistor by a linear method. We only show the water temperatures of 0–50 m in the CTL and CoLM-Lake runs because of the experimental settings. According to the observations in Lake Ontario (Figure 6d), the lake is isothermal in early spring, which keeps the water temperature less than 4 °C for the entire column. Then, the water temperature gradually increases and the stratification develops in June in response to the enhanced heating from the overlying atmosphere. During June to September, the lake temperature profile shows a warm upper mixed layer of 10 to 20 m thick and a cool lower layer, and the thickness of the mixed layer gradually increases. The depth of the 13 °C isotherm is usually defined as the thermocline position in Lake Ontario (Huang et al., 2010). A sharp thermocline is located at a depth of 20–25 m on day 165. The increased surface heat losses and enhanced vertical mixing, which is induced by strong winds, lead to the deepening of the thermocline from late September until the water column turns to a homogeneous thermal status. In addition, the water

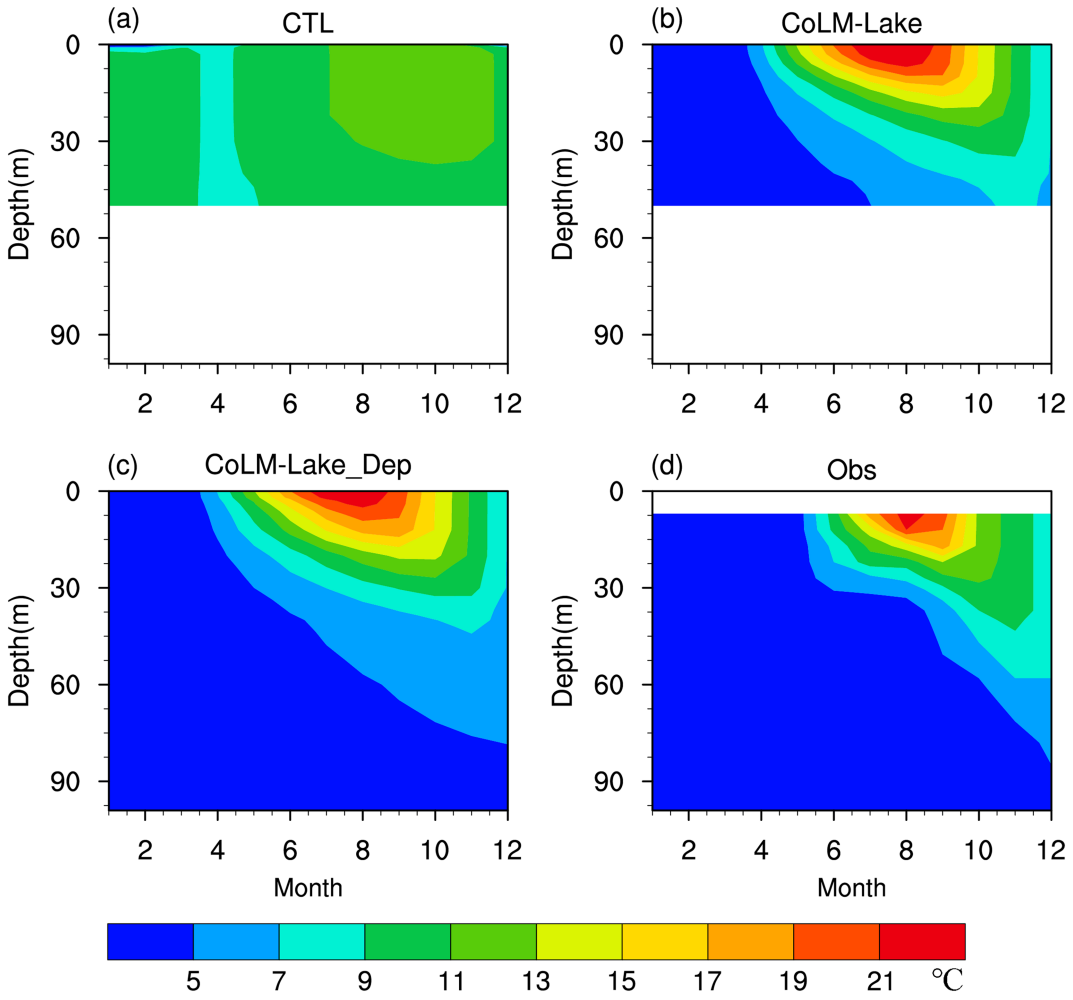

Figure 7. The modeled and observed monthly vertical water temperature profiles in south Michigan: (a) CTL, (b) CoLM-Lake, (c) CoLM-Lake_Dep, and (d) observation.

temperatures at the depths deeper than 50 m are mostly less than 6 °C (Huang et al., 2010). BCC_AVIM2.0 with the default lake scheme possesses a poor capability to simulate the temporal variation of the vertical temperature profile in the CTL run (Figure 6a). After the implementation of CoLM-Lake into BCC_AVIM2.0, the CoLM-Lake run shows a reasonable capability to simulate the vertical thermal structure and its seasonal evolution. The CoLM-Lake and CoLM-Lake_Dep runs generally produce very similar vertical profiles of water temperatures. However, both experiments produce gradual deepening of the thermocline and slight underestimation of the thickness of the upper mixed layer (Figures 6b and 6c). The CoLM-Lake run produces warmer water temperature biases at the upper layers shallower than 20 m in the early spring, and these biases slightly reduce in the CoLM-Lake_Dep run. This improvement is obtained by setting the real lake depth in this location, where the lake depth is more than 90 m.

The modeled and observed monthly vertical water temperature profiles in middle Lake Michigan are shown in Figure 7. Similar to the observations in Lake Ontario, the vertical temperature profile is poorly simulated by BCC_AVIM2.0 with the default lake scheme in the CTL run (Figure 7a). The implementation of the CoLM-Lake scheme can largely improve the model performance of BCC_AVIM2.0 in simulating the vertical thermal structure (Figure 7b). However, large biases can be also noted due to the lake depth setting to 50 m in the CoLM-Lake run at this location where the real lake depth is more than 100 m. Adopting the real lake depths in the CoLM-Lake_Dep run can further improve the simulations of the vertical water temperature profile (Figure 7c).

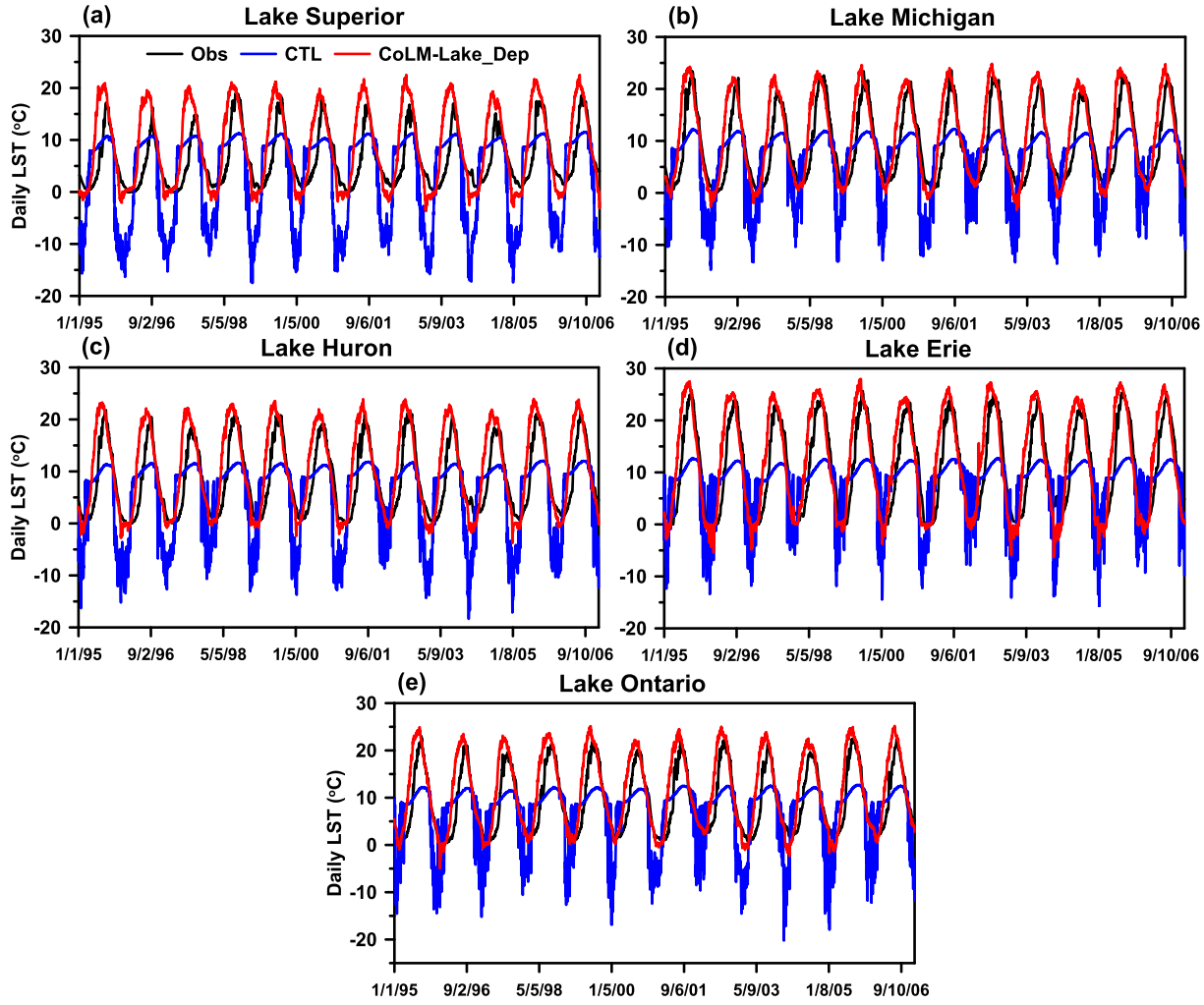

Figure 8. Time series of the daily LST regionally averaged over each lake of the Great Lakes from the GLSEA observation and the simulations of CTL and CoLM-Lake_Dep runs during 1995–2006.

Figure 8 gives the time series of the daily observed and modeled LST regionally averaged over each lake of the Great Lakes during 1995 to 2006. Compared to the observations, the CTL run produces large errors in the simulated LST and shows warm biases in spring and cold biases in other seasons, especially in winter. The statistic comparisons between the observed and simulated LST in each lake are shown in Figure 9. The RMSEs (temporal correlation coefficients) of modeled LST in the CTL run against the observation range from 6.8 to 8 °C (0.55 to 0.62), indicating the poor ability in capturing the seasonal variations and quantity of LST for all lakes. However, compared to the CTL run, the CoLM-Lake_Dep run produces much higher temporal correlation coefficient (lower RMSE). The temporal correlation coefficient increases by more than 30% for all lakes relative to that of CTL run, with the largest increase (~50%) in Ontario. In addition, the RMSEs of the modeled LST are significantly reduced by more than 30% for all lakes, indicating that replacing the default lake scheme with the CoLM lake scheme within BCC_AVIM2.0 leads to significant improvements in the temporal variation and magnitude of LST simulations over the Great Lakes region.

3.3. GST Over the Great Lakes Region

Our results demonstrate that adopting the CoLM-Lake scheme with the real lake depths can improve the performance of BCC_AVIM2.0 in simulating the spatial distribution and temporal variation of LST and vertical water temperature profile over the Great Lakes region. In this section, the effects of the lake on GST simulation, which strongly affects the air temperature in the coupled climate model, are further analyzed.

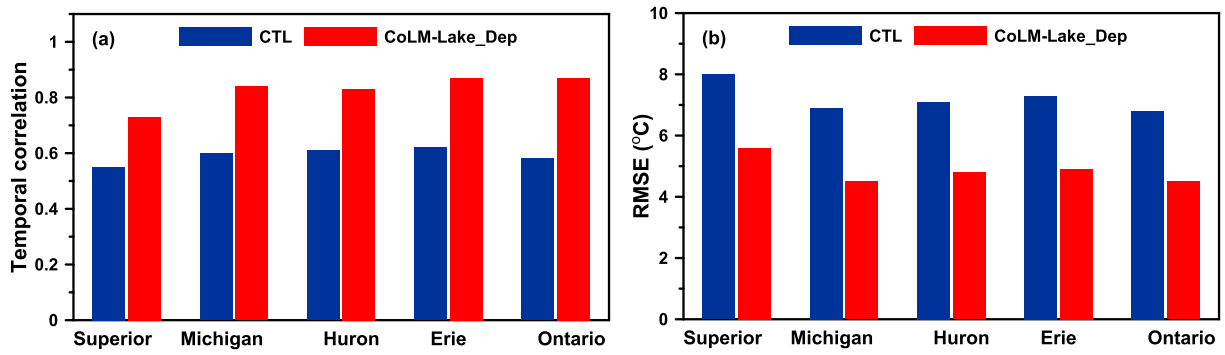

Figure 9. The (a) temporal correlation and (b) RMSE of the daily modeled LST regionally averaged over each lake of the Great Lakes in the CTL and CoLM-Lake_Dep runs against the GLSEA observation.

For land surface models, the GST is associated with an infinitesimal interface between the atmosphere and land surface for each grid. One grid may have different land cover types, such as lake, vegetation, and soil. And GST is described as

$$\mathrm{GST} = \sum_{i=1}^{n} f_i ST_i, \tag{4}$$

where i is the subgrid land type for a given model grid, and f_i and ST_i are the coverage fraction (%) and surface temperature of the ith subgrid land cover type at this model grid. If a grid has 100% lake coverage, then the GST is equal to the LST at this grid. We evaluate the GST simulations in the CTL run compared with the ERA reanalysis data. Figure 10 shows the GST biases produced by the CTL run over the Great Lakes region in winter and summer. Generally, the CTL run with the default lake scheme tends to underestimate the GST over the Great Lakes region in winter and summer. Much larger biases over the lake areas can be noted in winter (<−8 °C), which would bring large errors in the simulations

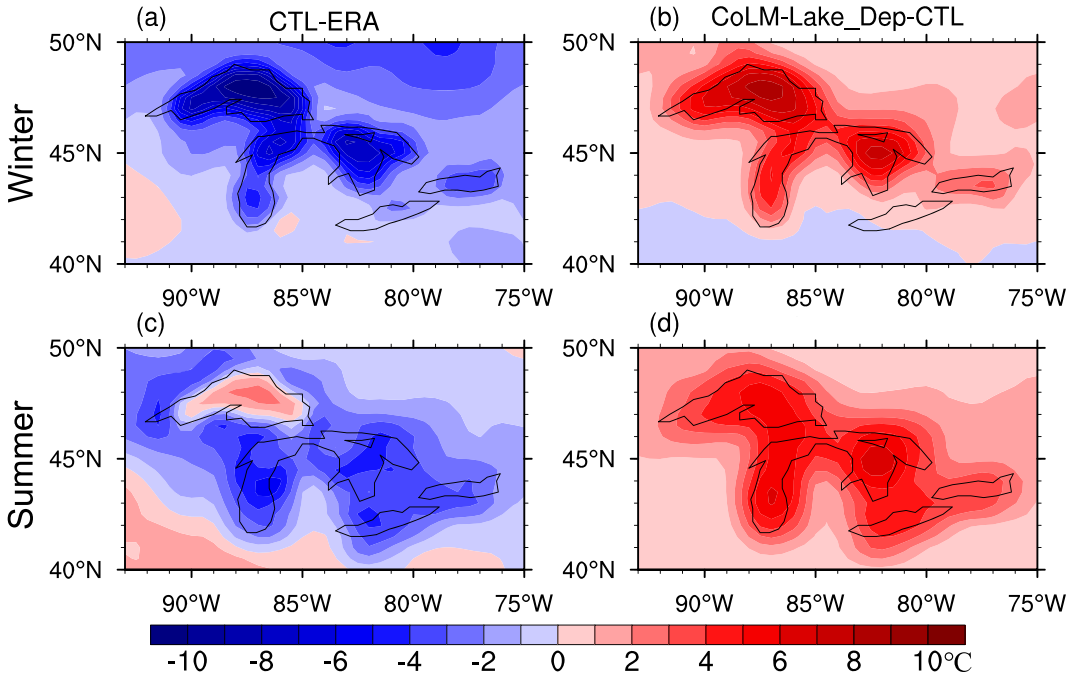

Figure 10. Differences of GST in (a, b) winter and (c, d) summer averaged over 1995–2006: (a, c) CTL minus ERA reanalysis and (b, d) CoLM-Lake_Dep minus CTL.

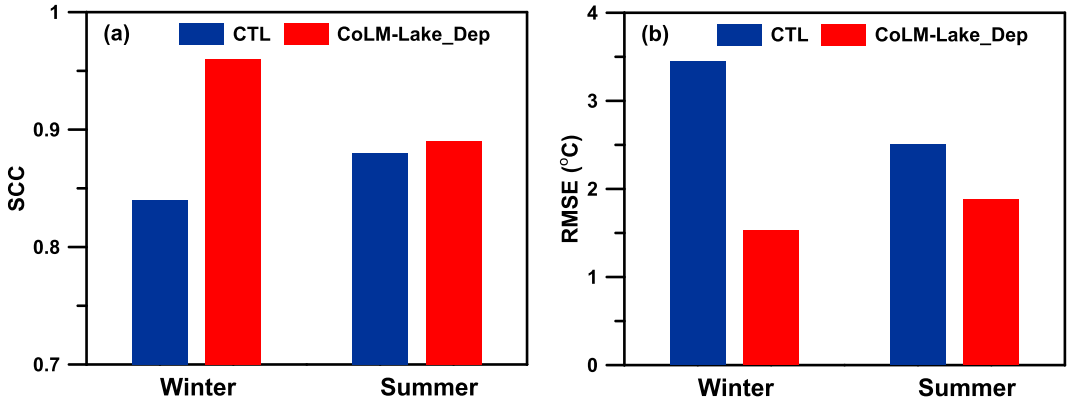

Figure 11. The (a) SCC and (b) RMSE of the modeled GST over the Great Lakes region in the CTL and CoLM-Lake_Dep runs against the ERA reanalysis.

of surface air temperature and precipitation around the Great Lakes in the coupled modeling system. From the GST differences between the CoLM-Lake_Dep and CTL runs (Figures 10b and 10d), adopting the CoLM-Lake scheme in BCC_AVIM2.0 can significantly reduce the GST biases in most of the Great Lakes region in winter and summer. The statistic comparisons between the observed and simulated GST over the Great Lakes region are shown in Figure 11. The RMSE of winter GST in the CoLM-Lake_Dep run has a substantial reduction by 56% compared to that in the CTL run. In addition, the SCC of GST produced by the CoLM-Lake_Dep run increases by 14% in winter over the Great Lakes region. The summer GST simulated in the CoLM-Lake_Dep run shows higher SCC and lower RMSE than that in the CTL run, similar to the winter results. The statistic comparisons indicate that adopting the CoLM-Lake scheme instead of the default lake scheme within BCC_AVIM2.0 can significantly reduce the GST biases over the Great Lakes region.

3.4. Lake Ice Over the Great Lakes Region

The evaluations of LST show that the performance of the CoLM-Lake scheme is largely improved in winter compared to that in the default lake scheme (Figure 3). The LST simulations are strongly affected by the process of ice formation. In the Great Lakes, ice cover typically lasts 3–5 months every year. The GLERL lake ice cover data are used to investigate the differences of lake ice formation between the CoLM-Lake and default lake schemes. Figure 12 gives the spatial distribution of the observed and modeled winter lake ice fraction over the Great Lakes. The lake ice cover fraction in Lake Erie is the highest among the five lakes. Lake Erie is the shallowest lake and has the lowest LST in winter (Figure 3). For the other lakes, the ice mainly appears along the lake shorelines. In the CTL run, the lake ice fraction is much higher than that of the GLERL observation, with the ice cover more than 50% in most of the Great Lakes (Figure 12b). The simulations from the CTL run indicate the poor performance of the default lake scheme in simulating lake ice in winter. The simulations of lake ice fraction are improved in the CoLM-Lake run compared to those in the CTL run. However, the values of lake ice fraction in the CoLM-Lake run are still higher than the observations due to the fixed lake depth of 50 m. The spatial distributions of lake ice are close to the GLERL observation, with higher (lower) ice fraction in the shallow (deep) lake in the CoLM-Lake_Dep run (Figure 12d). Figure 13 gives the multiple statistics of the simulated lake ice fraction in the Taylor diagram. The lake ice is poorly simulated in the CTL run, with the lowest SCC and largest RMSE among the three experiments. In addition, the SCC of lake ice fraction in the CoLM-Lake run is close to that of CTL, indicating the substantial impacts of lake depth on the lake ice simulations in winter. The spatial distributions of modeled lake ice are significantly improved by the CoLM-Lake_Dep run, with the values of SCC more than 0.5 for winter time. Overall, the performances of BCC_AVIM2.0 in simulating the lake ice in winter can be largely improved by replacing the default lake scheme with the CoLM-Lake scheme.

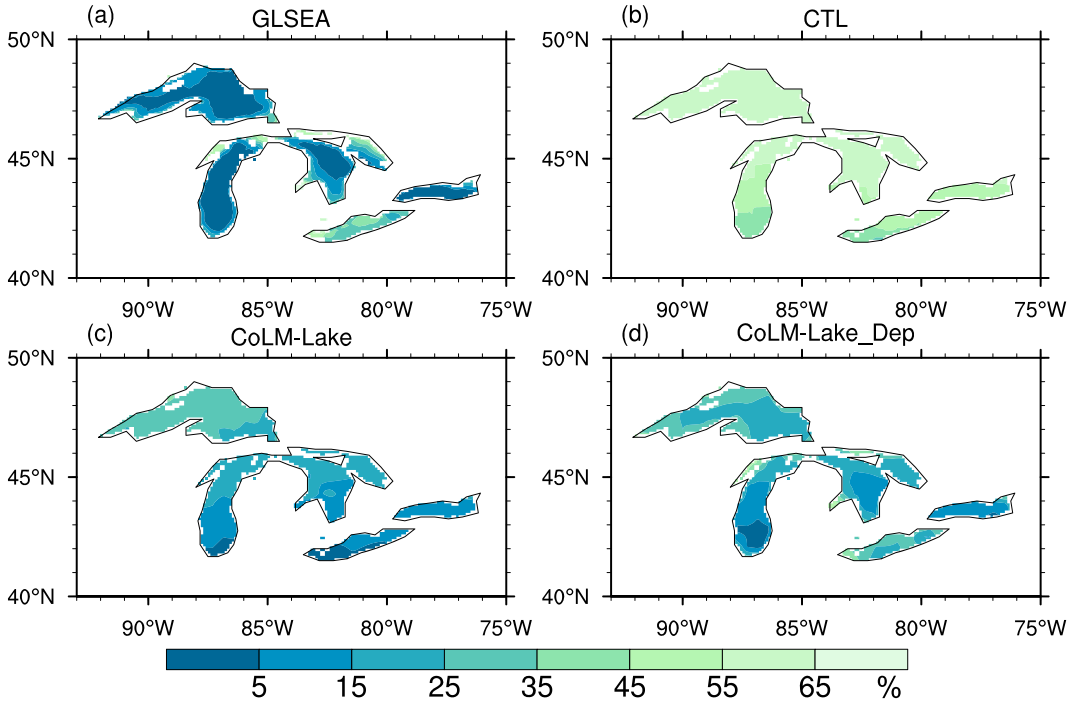

Figure 12. The observed and modeled lake ice fraction in winter (December, January, and February) averaged over 1999 to 2006. (a) GLSEA observation, (b) CTL, (c) CoLM-Lake, and (d) CoLM-Lake_Dep.

4. Discussion

4.1. Improvements and Uncertainties of the CoLM-Lake Scheme

In this study, we replaced the default lake scheme by the CoLM-Lake scheme in BCC_AVIM2.0 to improve the water temperature and GST simulations. BCC_AVIM2.0 with the CoLM-Lake scheme significantly improves the model performance in simulating the spatial pattern and seasonal variation of LST and thereafter the GST. BCC_AVIM2.0 with the updated lake scheme shows larger improvements in simulating the water temperatures during winter compared to those during other seasons, indicating the better descriptions of freezing-melting processes and the snow-ice-water heat exchanges in the CoLM-Lake scheme relative to the default lake scheme. The presence or absence of snow insulation may substantially delay the lake energy exchanges based on the model sensitivity results (Subin et al., 2012). However, the snow is not considered in the default lake scheme. These improved treatments of snow and ice may allow the CoLM-Lake scheme to have more realistic lake ice fraction and accurate prediction of temperature gradients in ice (Dai et al., 2018).

Vertical water mixing plays an important role in simulating LST and lake ice formation in winter (Huang et al., 2019). For the default lake scheme, the mixing is primarily contributed by wind-driven eddies. This type of water mixing may underestimate the mixing for deep lakes (Martynov et al., 2010; Perroud et al., 2009; Stepanenko et al., 2010), leading to weak seasonal variations of water temperature at deeper layers (Perroud et al., 2009). The CoLM_Lake scheme has three types of mixing to describe the mixing process: wind-driven eddy diffusion, molecular diffusion, and enhanced diffusion. Enhanced diffusion (K_{ed}), which is not considered in the default lake scheme, accounts for sources of turbulence induced by wave motions and horizontal temperature gradients. In the CoLM_Lake scheme, K_{ed} is described as

$$K_{ed} = 1.039 \times 10^{-8} \left(N^2\right)^{-0.43}, \tag{5}$$

$$N^2 = \frac{g}{\rho_i} \frac{\rho_{i+1}{}^{-i+1}\rho_i}{z_{i+1} - z_i} \geq 7.5 \times 10^{-5}, \tag{6}$$

where g is the acceleration of gravity and ρ_i and z_i are the water density and depth of the ith layer,

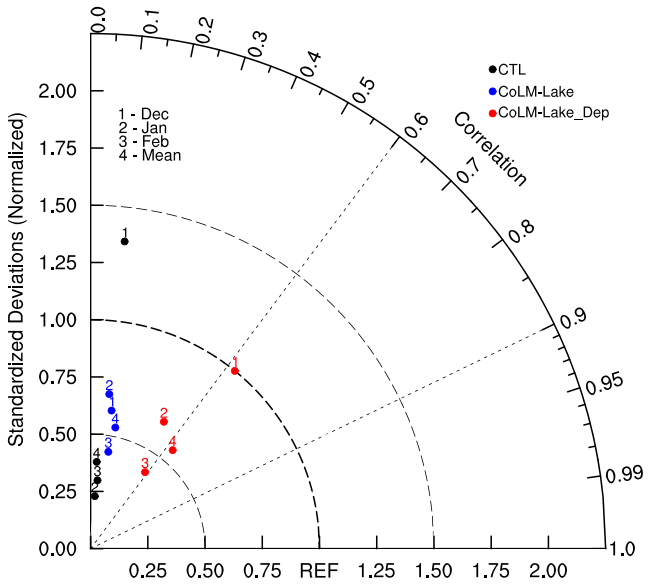

Figure 13. Taylor diagram of the lake ice fraction simulation against GLSEA observation over the Great Lakes region. The simulations in December, January, and February and winter mean are denoted by numbers; the black, blue, and red marks denote the simulations from the CTL, CoLM-Lake, and CoLM-Lake_Dep experiments, respectively.

respectively. For the frozen lakes, enhanced diffusion is important for the water mixing because of the absence of wind-driven eddy diffusion (Dai et al., 2018). Our results show that the vertical water mixing in the CTL run is very weak, leading to the cold bias of LST and higher lake ice fraction in winter (Figures 3 and 12). However, the water mixing in the CoLM-Lake_Dep run is closer to the observations than that in the CTL run, and the spatial patterns of LST and lake ice agree well with the observations over the Great Lakes. These improvements of the LST and lake ice simulations in the CoLM_Lake scheme indicate the prolonged impacts of the water mixing pattern on the thermal structure in lake schemes.

Even though the CoLM-Lake scheme has substantial improvements over the Great Lakes region, it still produces an early and quick warming of LST in late spring and early summer. The LST biases vary among the five lakes. The simulated LST is close to the observations for Lake Erie, while the LST is much warmer than the observation over Lake Superior (Figure 8). Generally, most of the current 1-D lake models tend to produce better seasonal evolution of LST in shallow lakes than in deep lakes (Xiao et al., 2016). Although the CoLM-Lake scheme has improvements of water mixing in winter, it still has insufficient mixing in summer. Increasing the eddy diffusivity can delay the earlier warm-up in spring and can produce much closer LST simulations with the observations for deep lakes (Gu et al., 2015; Huang et al., 2019). In addition, the extinction coefficient is an important parameter for LST simulations. The extinction coefficient varies with lake depth in the CoLM-Lake scheme. Actually, the value of the extinction coefficient also depends on water clarity and quality. Potes et al. (2012) found that water clarity is an essential parameter affecting the LST simulations. Moreover, the extinction coefficient derived from satellite data has obvious spatial variations in Lake Erie (Zolfaghari et al., 2017). In the future, the satellite-derived extinction coefficient products can be used to improve the performance of the lake models.

4.2. Effects of Lakes on Regional Climate

Lake-atmosphere interactions have substantial influences on climates from local to regional scales (Sharma et al., 2018). Many studies have been conducted to investigate the importance of lake-atmosphere interaction in the regional climate models, which are coupled with lake parameterizations (Lofgren, 1997; Steenburgh & Campbell, 2017; Veals & Steenburgh, 2015). Wu et al. (2019) examined the lake effects on the local climate over the Tibetan Plateau in summer and demonstrated that the alpine lakes tend to cool the local air temperature and enhance the precipitation over the lake and surrounding areas. Diallo et al. (2018) found that the increased evaporation of the lake, combining with enhanced rising motions and low-level moisture convergence, resulted in more precipitation over a tropical lake and neighboring areas based on the simulations from a regional climate model. Our results also confirm that the lake have a profound influence on GST over the Great Lakes region. The offline simulations from BCC_AVIM2.0 indicate that the performances in simulating the GST are significantly improved by adopting the CoLM-Lake scheme instead of the default lake scheme, especially during the winter. To investigate the lake effects on local and regional climates, some analyses based on the simulations from the land-atmosphere coupled model are shown in this paper. Two numerical experiments using the coupled model are conducted here. In the CTL_coupled run, all the settings of the lake scheme are the same as those in the CTL run. In the CoLM_coupled run, all the settings of the lake scheme are the same as those in the CoLM-Lake_Dep run. The air temperature and precipitation in winter are shown here (Figure 14) due to the large improvements of simulating winter LST. Figure 14a shows the biases of air temperature in the CTL_coupled run over the Great Lakes region. The air temperature in winter is largely underestimated over the Great Lakes region in the CTL_coupled run. The differences between the CoLM_coupled and CTL_coupled runs show that the cold biases of air temperature are significantly reduced by adopting the CoLM-Lake scheme in the coupled model over the Great Lakes region (Figures 14b). The simulations of precipitation are also improved in most of the Great Lakes region in the

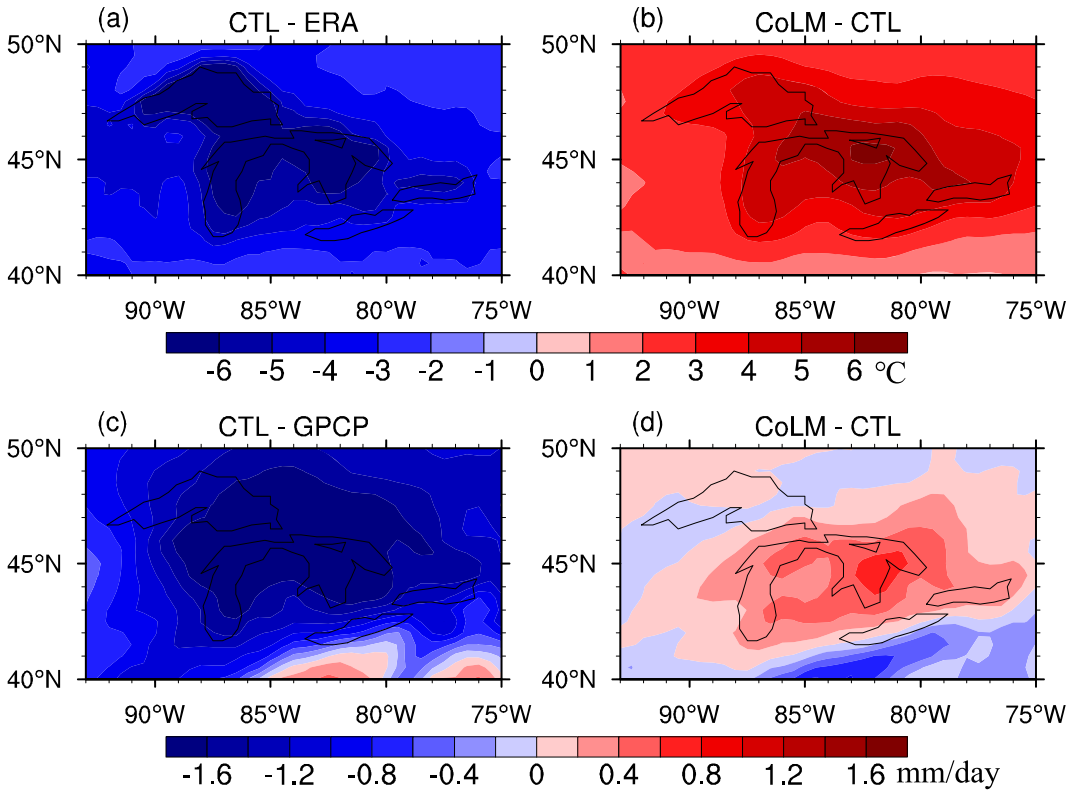

Figure 14. Differences of (a, b) 2 m air temperature and (c, d) precipitation in winter from the coupled model: (a, c) CTL_coupled minus reanalysis data and (b, d) CoLM_coupled minus CTL_coupled.

CoLM_coupled run (Figures 14c and 14d), especially over the lake area. The simulations of air temperature and precipitation from the coupled model demonstrate that the lake has substantial impacts on local and regional climates and a more realistic lake scheme can improve the lake-atmosphere interactions in climate models.

5. Conclusions

In this paper, the default lake scheme within the BCC_AVIM2.0 land surface model is replaced by the CoLM-Lake scheme to improve the spatial and temporal variability of LST, vertical profile of water temperature evolution, and the spatial distribution of the GST over the Great Lakes region. BCC_AVIM2.0 with the default lake scheme shows poor ability to simulate the spatial and temporal variability of LST. In winter, the cold LST biases produced by the default lake scheme can be largely reduced by adopting the CoLM-Lake scheme, in which the simulations of the vertical water temperature profile are largely improved. Much larger improvements in simulating LST, lake ice fraction, and water temperature profiles in winter indicate better descriptions of freezing-melting processes and the snow-ice-water heat exchanges in the CoLM-Lake scheme. Furthermore, the improvements of the LST simulated by BCC_AVIM2.0 with the adoption of the CoLM-Lake scheme significantly reduce the GST biases produced by BCC_AVIM2.0 with the adoption of the default lake scheme. Even though the new lake scheme exhibits some substantial improvements over the Great Lakes region, it still produces rapid warming of LST in late spring and early summer, especially for deep lakes. This warm LST bias may be caused by the insufficient water mixing in spring and summer. The simulations from land-atmosphere coupled model confirm that the air temperature and precipitation are also improved by adopting the CoLM-Lake scheme, which has better performance of simulating the energy and water exchange between atmosphere and lakes. This study highlights the importance of a more realistic lake scheme land surface model, which can describe much more realistic lake-atmosphere interactions over lake-rich regions in the future.

Acknowledgments

This work was supported by the National Key R&D Program of China under grants 2017YFA0604300 and 2016YFA0602602; the National Natural Science Foundation of China under grants 41975081, 91537102, and 41705056; the Jiangsu University "Blue Project" outstanding young teachers training object; the Natural Science Foundation of Jiangsu Province (BK20170638); the Fundamental Research Funds for the Central Universities; and the Jiangsu Collaborative Innovation Center for Climate Change. The authors acknowledge the National Oceanic and Atmospheric Administration Great Lakes Surface Environmental Analysis for the lake data sets (https://coastwatch.glerl.noaa.gov/glsea/glsea.html) and the European Center for Medium-range Weather Forecasts for the reanalysis data (https://apps.ecmwf.int/datasets/data/interim-full--moda/levtype=sfc/). We also thank the three anonymous reviewers for their constructive comments and suggestions.

References

Adler, R. F., Huffman, G. J., Chang, A., Ferraro, R., Xie, P. P., Janowiak, J., et al. (2003). The version-2 Global Precipitation Climatology Project (GPCP) monthly precipitation analysis (1979–present). *Journal of Hydrometeorology*, *4*(6), 1147–1167. https://doi.org/10.1175/1525-7541(2003)004<1147:TVGPCP>2.0.CO;2

Bonan, G. B., Oleson, K. W., Vertenstein, M., Levis, S., Zeng, X., Dai, Y., et al. (2002). The land surface climatology of the community land model coupled to the NCAR community climate model. *Journal of Climate*, *15*(22), 3123–3149. https://doi.org/10.1175/1520-0442(2002)015<3123:TLSCOT>2.0.CO;2

Charusombat, U., Fujisaki-Manome, A., Gronewold, A. D., Lofgren, B. M., Anderson, E. J., Blanken, P. D., et al. (2018). Evaluating and improving modeled turbulent heat fluxes across the north American Great Lakes. *Hydrology and Earth System Sciences*, *22*(10), 5559–5578. https://doi.org/10.5194/hess-22-5559-2018

Choulga, M., Kourzeneva, E., Zakharova, E., & Doganovsky, A. (2014). Estimation of the mean depth of boreal lakes for use in numerical weather prediction and climate modelling. *Tellus A: Dynamic Meteorology and Oceanography*, *66*(1), 21295. https://doi.org/10.3402/tellusa.v66.21295

Dai, Y., Wei, N., Huang, A., Zhu, S., Shangguan, W., Yuan, H., et al. (2018). The lake scheme of the common land model and its performance evaluation (Chinese with English abstract). *Chinese Science Bulletin*, *63*(28-29), 3002–3021. https://doi.org/10.1360/N972018-00609

Dai, Y., Zeng, X., Dickinson, R. E., Baker, I., Bonan, G. B., Bosilovich, M. G., et al. (2003). The common land model. *Bulletin of the American Meteorological Society*, *84*(8), 1013–1024. https://doi.org/10.1175/BAMS-84-8-1013

Diallo, I., Giorgi, F., & Stordal, F. (2018). Influence of Lake Malawi on regional climate from a double-nested regional climate model experiment. *Climate Dynamics*, *50*(9-10), 3397–3411. https://doi.org/10.1007/s00382-017-3811-x

Goyette, S., McFarlane, N. A., & Flato, G. M. (2000). Application of the Canadian regional climate model to the Laurentian Great Lakes region: Implementation of a lake model. *Atmosphere-Ocean*, *38*(3), 481–503. https://doi.org/10.1080/07055900.2000.9649657

Gu, H., Jin, J., Wu, Y., Ek, M. B., & Subin, Z. M. (2015). Calibration and validation of LST simulations the coupled WRF-lake model. *Climatic Change*, *129*(3-4), 471–483. https://doi.org/10.1007/s10584-013-0978-y

Gula, J., & Peltier, W. R. (2012). Dynamical downscaling over the Great Lakes basin of North America using the WRF regional climate model: The impact of the Great Lakes system on regional greenhouse warming. *Journal of Climate*, *25*(21), 7723–7742. https://doi.org/10.1175/JCLI-D-11-00388.1

Hostetler, S. W., & Bartlein, P. J. (1990). Simulation of lake evaporation with application to modeling lake level variations of Harney-Malheur Lake, Oregon. *Water Resources Research*, *26*(10), 2603–2612.

Huang, A., Rao, Y., & Lu, Y. (2010). Evaluation of a 3D hydrodynamic model and atmospheric forecast forcing using observations in Lake Ontario. *Journal of Geophysical Research*, *115*, C02004. https://doi.org/10.1029/2009jc005601

Huang, A., Wang, J., Dai, Y., Yang, K., Wei, N., Wen, L., et al. (2019). Evaluating and improving the performance of three 1-D Lake models in a large deep Lake of the central Tibetan Plateau. *Journal of Geophysical Research*, *124*, 3143–3167. https://doi.org/10.1029/2018JD029610

Ji, J. (1995). A climate-vegetation interaction model: Simulating physical and biological processes at the surface. *Journal of Biogeography*, *22*, 2063–2069.

Ji, J., Huang, M., & Li, K. (2008). Prediction of carbon exchange between China terrestrial ecosystem and atmosphere in 21st century. *Science in China Series D: Earth Sciences*, *51*(6), 885–898. https://doi.org/10.1007/s11430-008-0039-y

Li, W., Zhang, Y., Shi, X., Zhou, W., Huang, A., Mu, M., & Qiu, B. (2019). Development of land surface model BCC_AVIM2.0 and its preliminary performance in LS3MIP/CMIP6. *Journal of Meteorological Research*, *33*(5), 851–869. https://doi.org/10.1007/s13351-019-9016-y

Lofgren, B. M. (1997). Simulated effects of idealized Laurentian Great Lakes on regional and large-scale climate. *Journal of Climate*, *10*, 2847–2858.

Mallard, M. S., Nolte, C. G., Bullock, O. R., Spero, T. L., & Gula, J. (2014). Using a coupled lake model with WRF for dynamical downscaling. *Journal of Geophysical Research*, *119*, 7193–7208. https://doi.org/10.1002/2014JD021785

Martynov, A., Sushama, L., & Laprise, R. (2010). Simulation of temperate freezing lakes by one-dimensional lake models: Performance assessment for interactive coupling with regional climate models. *Boreal Environment Research*, *15*, 143–164.

Mironov, D., Rontu, L., Kourzeneva, E., & Terzhevik, A. (2010). Towards improved representation of lakes in numerical weather prediction and climate models: Introduction to the special issue of boreal environment research. *Boreal Environment Research*, *15*, 97–99.

Norton, D. C., & Bolsenga, S. J. (1993). Spatiotemporal trends in lake effect and continental snowfall in the Laurentian Great Lakes, 1951–1980. *Journal of Climate*, *6*(10), 1943–1956. https://doi.org/10.1175/1520-0442(1993)006<1943:STILEA>2.0.CO;2

Notaro, M., Zarrin, A., Vavrus, S., & Bennington, V. (2013). Simulation of heavy lake-effect snowstorms across the Great Lakes basin by RegCM4: Synoptic climatology and variability. *Monthly Weather Review*, *141*(6), 1990–2014. https://doi.org/10.1175/MWR-D-11-00369.1

Patz, J. A., Vavrus, S. J., Uejio, C. K., & McLellan, S. L. (2008). Climate change and waterborne disease risk in the Great Lakes region of the US. *American Journal of Preventive Medicine*, *35*(5), 451–458. https://doi.org/10.1016/j.amepre.2008.08.026

Perroud, M., Goyette, S., Martynov, A., Beniston, M., & Annevillec, O. (2009). Simulation of multiannual thermal profiles in deep Lake Geneva: A comparison of one-dimensional lake models. *Limnology and Oceanography*, *54*(5), 1574–1594. https://doi.org/10.4319/lo.2009.54.5.1574

Potes, M., Costa, M. J., & Salgado, R. (2012). Satellite remote sensing of water turbidity in Alqueva reservoir and implications on lake modelling. *Hydrology and Earth System Sciences*, *16*(6), 1623–1633. https://doi.org/10.5194/hess-16-1623-2012

Qiu, B., Guo, W., Xue, Y., & Dai, Q. (2016). Implementation and evaluation of a generalized radiative transfer scheme within canopy in the soil-vegetation-atmosphere transfer (SVAT) model. *Journal of Geophysical Research*, *121*, 12,145–12,163. https://doi.org/10.1002/2016JD025328

Schwab, D., Leshkevich, G., & Muhr, G. (1992). Satellite measurements of surface water temperature in the Great Lakes: Great Lakes Coastwatch. *Journal of Great Lakes Research*, *18*(2), 247–258. https://doi.org/10.1016/S0380-1330(92)71292-1

Sharma, A., Hamlet, A. F., Fernando, H. J. S., Catlett, C. E., Horton, D. E., Kotamarthi, V. R., et al. (2018). The need for an integrated land-lake-atmosphere modeling system, exemplified by North America's Great Lakes region. *Earth's Future*, *6*, 1366–1379. https://doi.org/10.1029/2018EF000870

Sheffield, J., Goteti, G., & Wood, E. F. (2006). Development of a 50-year high-resolution global dataset of meteorological forcings for land surface modeling. *Journal of Climate*, *19*(13), 3088–3111. https://doi.org/10.1175/JCLI3790.1

Steenburgh, W. J., & Campbell, L. S. (2017). The OWLeS IOP2b lake-effect snowstorm: Shoreline geometry and the mesoscale forcing of precipitation. *Monthly Weather Review*, *145*(7), 2421–2436. https://doi.org/10.1175/MWR-D-16-0460.1

Stepanenko, V. M., Goyette, S., Martynov, A., Perroud, M., Fang, X., & Mironov, D. (2010). First steps of a Lake Model Intercomparison Project: LakeMIP. *Boreal Environment Research*, *15*, 191–202.

Subin, Z. M., Riley, W. J., & Mironov, D. (2012). An improved lake model for climate simulations: Model structure, evaluation, and sensitivity analyses in CESM1. *Journal of Advances in Modeling Earth Systems*, *4*, M02001. https://doi.org/10.1029/2011ms000072

Taylor, K. E. (2001). Summarizing multiple aspects of model performance in a single diagram. *Journal of Geophysical Research*, *106*(D7), 7183–7192. https://doi.org/10.1029/2000JD900719

Veals, P. G., & Steenburgh, W. J. (2015). Climatological characteristics and orographic enhancement of lake-effect precipitation east of Lake Ontario and over the Tug Hill Plateau. *Monthly Weather Review*, *143*(9), 3591–3609. https://doi.org/10.1175/MWR-D-15-0009.1

Wu, T., Li, W., Ji, J., Xin, X., Li, L., Wang, Z., et al. (2013). Global carbon budgets simulated by the Beijing Climate Center Climate System Model for the last century. *Journal of Geophysical Research*, *118*, 4326–4347. https://doi.org/10.1002/jgrd.50320

Wu, T., Lu, Y., Fang, Y., Xin, X., Li, L., Li, W., et al. (2019). The Beijing Climate Center Climate System Model (BCC-CSM): The main progress from CMIP5 to CMIP6. *Geoscientific Model Development*, *12*(4), 1573–1600. https://doi.org/10.5194/gmd-12-1573-2019

Wu, T., Song, L., Li, W., Wang, Z., Zhang, H., Xin, X., et al. (2014). An overview of BCC climate system model development and application for climate change studies. *Journal of Meteorological Research*, *28*(1), 34–56.

Wu, T., Yu, R., Zhang, F., Wang, Z., Dong, M., Wang, L., et al. (2010). The Beijing Climate Center atmospheric general circulation model: Description and its performance for the present-day climate. *Climate Dynamics*, *34*(1), 123–147. https://doi.org/10.1007/s00382-008-0487-2

Wu, Y., Huang, A., Yang, B., Dong, G., Wen, L., Lazhu, et al. (2019). Numerical study on the climatic effect of the lake clusters over Tibetan Plateau in summer. *Climate Dynamics*, *53*(9-10), 5215–5236. https://doi.org/10.1007/s00382-019-04856-4

Xiao, C., Lofgren, B. M., Wang, J., & Chu, P. Y. (2016). Improving the lake scheme within a coupled WRF-lake model in the Laurentian Great Lakes. *Journal of Advances in Modeling Earth Systems*, *8*, 1969–1985. https://doi.org/10.1002/2016MS000717

Xin, X., Wu, T., & Zhang, J. (2013). Introduction of CMIP5 experiments carried out with the climate system models of Beijing Climate Center. *Advances in Climate Change Research*, *4*(1), 41–49. https://doi.org/10.3724/SP.J.1248.2013.00041

Zeng, X., Shaikh, M., Dai, Y., Dickinson, R., & Myneni, R. (2002). Coupling of the common land model to the NCAR community climate model. *Journal of Climate*, *15*(14), 1832–1854. https://doi.org/10.1175/1520-0442(2002)015<1832:COTCLM>2.0.CO;2

Zhou, W., Luo, Y., Li, W., Shi, X., & Zhang, Y. (2018). Comparative studies of different radiation schemes within vegetation in land model (Chinese with English abstract). *Chinese Science Bulletin*, *63*, 2772–2784.

Zolfaghari, K., Duguay, C. R., & Kheyrollah Pour, H. (2017). Satellite-derived light extinction coefficient and its impact on thermal structure simulations in a 1-D lake model. *Hydrology and Earth System Sciences*, *21*(1), 377–391. https://doi.org/10.5194/hess-21-377-2017